Deformation Crossover: From Nano- to Mesoscale

S. Cheng,[1,2] A. D. Stoica,[1] X.-L. Wang,[1,*] Y. Ren,[3] J. Almer,[3] J. A. Horton,[4] C. T. Liu,[4,5] B. Clausen,[6] D. W. Brown,[6] P. K. Liaw,[2] and L. Zuo[7]

[1]*Neutron Scattering Science Division, Oak Ridge National Laboratory, Oak Ridge, Tennessee 37831, USA*
[2]*Department of Materials Science and Engineering, The University of Tennessee, Knoxville, Tennessee 37996, USA*
[3]*X-ray Science Division, Argonne National Laboratory, Argonne, Illinois 60439, USA*
[4]*Materials Science and Technology Division, Oak Ridge National Laboratory, Oak Ridge, Tennessee 37831, USA*
[5]*Mechanical Engineering Department, Hong Kong Polytechnic University, Hung Tom, Kowloon, Hong Kong*
[6]*Los Alamos Neutron Science Center, Los Alamos National Laboratory, Los Alamos, New Mexico 87545, USA*
[7]*Key Laboratory for Anisotropy and Texture of Materials (Ministry of Education), Northeastern University, Shenyang 110004, People's Republic of China*

(Received 7 September 2008; published 17 July 2009)

In situ synchrotron and neutron diffraction were used to study deformation mechanisms in Ni over a broad range of grain sizes. The experimental data show that unlike in coarse-grained metals, where the deformation is dominated by dislocation slip, plastic deformation in nanocrystalline Ni is mediated by grain-boundary activities, as evidenced by the lack of intergranular strain and texture development. For ultrafine-grained Ni, although dislocation slip is an active deformation mechanism, deformation twinning also plays an important role, whose propensity increases with the grain size.

DOI: 10.1103/PhysRevLett.103.035502 PACS numbers: 62.20.F−, 61.05.C−, 61.05.F−, 62.25.−g

Introduction.—Recent studies of the mechanical behavior of nanocrystalline (NC) metals have generated considerable debate over deformation mechanisms at small length scales [1–12]. It has been widely anticipated that when the grain size is reduced to the nanometer regime, the deformation is no longer dominated by dislocation, as the critical shear stress needed to initiate the dislocation is inversely proportional to the grain size [9,12]. Shear transformation (e.g., deformation twinning) is another way some metals deform. However, the nucleation of twinning usually requires a very high local stress concentration or special heterogeneities [13]. Alternate deformation mechanisms, such as grain-boundary (GB) mediated plasticity, have been proposed, but with little experimental substantiation. For example, molecular dynamics (MD) simulations suggest that GB-mediated deformation (e.g., GB sliding) becomes prominent in Ni with a grain size $D \leq 10$ nm [4]. Stacking faults via partial dislocation emission were also predicted in Ni with $D \sim 20$ nm [5]. However, subsequent *in situ* synchrotron x-ray measurements showed no evidence of stacking faults; instead, a reversible peak broadening was reported during loading/unloading, which was attributed to the lack of buildup of a residual dislocation network after the plastic deformation [11]. A recent *in situ* synchrotron loading experiment in NC Ni containing 15 wt.% Fe revealed a tensile deflection in the lattice strains. This was attributed to localized deformation in a hypothetical ''soft grain-boundary region'' [14]. Unfortunately, the interpretation of these experimental data is complicated by the significant alloy addition. Indeed, chemical segregation may lead to a soft grain-boundary phase of a different chemical makeup. For solid-solution alloys, it is also well known that the critical shear stress is a sensitive function of alloy compositions. In Ag-Al, for example, the critical shear stress increases by 1 order of magnitude with 6 at. % of Al [15]. In addition, significant growth twins were observed in Ni-Fe alloys, due to a lower stacking fault energy cause by Fe addition [16], whose effect on the lattice strain has not been clarified. It is also difficult to compare these experimental strain data with theoretical calculations as present theories ignore the effect of alloying. Thus, the nature of plastic deformation in NC materials remains unclear, and the fundamental question as to whether a crossover exists from the traditional dislocation slip to GB-mediated deformation lingers. In this Letter, we report a critical examination of the plastic deformation in pure Ni from the perspective of intergranular strain and texture evolution by *in situ* loading experiments with high-energy synchrotron x-ray and neutron diffraction. NC and ultra-fine-grained (UFG) Ni samples were investigated, and significantly different deformation behaviors were observed.

Experimental method and data analysis.—In polycrystalline metals subjected to uniaxial loading, the lattice strain response within a grain, which can be readily measured by neutron or x-ray diffraction, depends on the grain orientation. In the elastic regime, the lattice strain is linear and scales with the elastic anisotropy. When plastic deformation occurs, however, the lattice strain starts to deviate from the linear elastic response. The additional elastic strain that develops in the grains to accommodate inhomogeneous plastic deformation during the macroscopic elasto-plastic transition is termed the intergranular or type II strain, $\varepsilon_{\mathrm{II}}^{hkl}$, where the superscript denotes grains with (hkl) planes normal to the direction of measurement (specified by the scattering vector) [17]. Signature $\varepsilon_{\mathrm{II}}^{hkl}$

develops due to the activation of select slip planes. In coarse-grained (CG) *fcc* metals under tensile deformation, for example, a tensile and compressive intergranular strains develop in ⟨200⟩//LD and ⟨220⟩//LD grains, respectively [17], where LD designates the loading direction. This is a direct result of the crystal elastic and plastic anisotropy [18–20]. The ⟨111⟩//LD grains, on the other hand, show a minimal intergranular strain. Meanwhile, a characteristic texture also develops during deformation as grains rotate toward ⟨111⟩//LD and to a lesser extent toward ⟨200⟩//LD while the population of ⟨220⟩//LD grains is depleted [17–19,21].

Thus, *in situ* loading studies of the intergranular strain and texture evolution provide unique insights and have been used as fingerprints for understanding deformation behaviors. Neutron and high-energy synchrotron radiation are highly penetrating for most engineering materials, ensuring that the measurements are representative of the bulk. Additionally, the scattering geometry with neutron and high-energy synchrotron measurements allows easy access of ${\varepsilon_{\rm II}}^{hkl}$ for desired grain orientations.

Ni samples of 99.5% purity with different grain sizes were obtained from Integran Technologies, Inc. (Canada). The as-received samples contained no preexisting twins, as confirmed by transmission electron microscopy (TEM). Three samples were studied by *in situ* synchrotron and neutron diffraction, with a nominal grain size of 20 (*A*), 100 (*B*), and 1000 (*C*) nm. Lattice strain data were collected in stepwise scans during quasistatic loading and unloading (with a strain rate of $\sim 10^{-5}$ s^{-1}). The stress-strain curves from the synchrotron experiments are shown in Fig. 1(a).

The evolution of intergranular strain and texture was quantified using two index parameters. For each reflection (*hkl*), an intergranular strain index is defined as $\Delta^{hkl} = \langle|{\varepsilon_{\rm II}}^{hkl}|\rangle_\psi = \langle|{\varepsilon_{\rm exp}}^{hkl} - {\varepsilon_{\rm cal}}^{hkl}|\rangle_\psi$, where ψ is the azimuthal angle between the scattering vector and LD, and $|{\varepsilon_{\rm exp}}^{hkl} - {\varepsilon_{\rm cal}}^{hkl}|$ describes the deviation of the experimental strain value from the linear elastic behavior. The texture index is defined similarly, $\Pi^{hkl} = \langle|{I_{\rm exp}}^{hkl} - {I_{\rm ref}}^{hkl}|\rangle_\psi$, where ${I_{\rm ref}}^{hkl}$ is the reference intensity before loading.

Results.—Figure 1(b) shows $\langle\Delta^{hkl}\rangle$, the intergranular strain index Δ^{hkl} averaged over the first three diffraction peaks: (111), (200), and (220). For all samples, small residual stresses were present, but they were quickly relaxed after initial loading. As the plastic deformation proceeded, completely different loading behaviors were observed in NC and UFG samples. Significant ${\varepsilon_{\rm II}}^{hkl}$ develops in UFG samples *B* and *C*, which increases with increasing plastic deformation. In stark contrast, NC sample *A* showed little ${\varepsilon_{\rm II}}^{hkl}$ development up to 3% of macroscopic strain, corresponding to about 2% of plastic strain, as shown in the inset of Fig. 1(b).

The contrasting deformation behaviors were also manifested in the texture development, as illustrated in Fig. 1(c) with $\langle\Pi^{hkl}\rangle$ (again, averaged over the first three

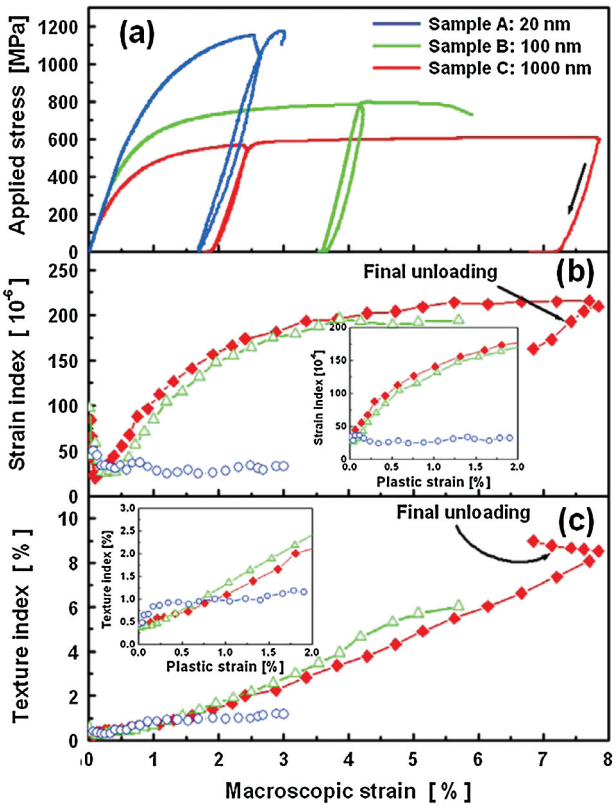

FIG. 1 (color). (a) Macroscopic stress-strain curves of three Ni samples measured during *in situ* synchrotron diffraction experiments. (b) The intergranular strain index $\langle\Delta^{hkl}\rangle$ and (c) the texture index $\langle\Pi^{hkl}\rangle$ of Ni samples as a function of macroscopic strain. Both indices are average values over the first three reflections (111), (200), and (220). The insets show $\langle\Delta^{hkl}\rangle$ and $\langle\Pi^{hkl}\rangle$ as a function of the plastic strain. For each sample, two loading cycles are demonstrated. Samples *A* and *B* broke during the second load. For sample *C*, $\langle\Delta^{hkl}\rangle$ showed some relaxation after the second unload.

reflections). The variation of $\langle\Pi^{hkl}\rangle$ during elastic deformation indicates the level of measurement precision. A linear growth is seen for $\langle\Pi^{hkl}\rangle$ of UFG samples, whereas for the NC sample, the $\langle\Pi^{hkl}\rangle$ was nearly constant during plastic deformation, except for a small jump at the beginning. Notice that ${\varepsilon_{\rm II}}^{hkl}$ stayed at minimum throughout the deformation process. Thus, while the small jump suggests that slight grain rotations might have occurred at the onset of plastic deformation in NC Ni, the constant texture index thereafter confirms the lack of dislocation activities during plastic deformation, which would have induced a steady rotation of grains. Together, the evolution of intergranular strain and texture provided clear evidence that, unlike in CG Ni, plastic deformation in NC Ni is limited to the grain boundaries as Ni grains deformed only elastically.

The texture developed in the UFG Ni is characterized by the strong buildup of ⟨111⟩//LD, a moderate increase of ⟨200⟩//LD, and depletion of ⟨220⟩//LD, which is typical of the tensile texture due to dislocation slip, as in CG Ni [17–19,21]. As to ${\varepsilon_{\rm II}}^{hkl}$, although significant ${\varepsilon_{\rm II}}^{hkl}$ was

observed, the ψ dependence of ε_{II}^{hkl} for samples *B* and *C* do not behave the same as their CG counterparts. For example, the residual ε_{II}^{200} (after unloading) was tensile in the transverse direction (TD), but compressive in LD. The latter observation, which was also verified by our *in situ* neutron diffraction experiment, is markedly different from the behavior of CG *fcc* metals, where a tensile ε_{II}^{200} appears in both LD and TD, with a somewhat higher value in LD [18–20]. Figure 2(a) summarizes residual ε_{II}^{200} from *in situ* neutron and x-ray measurements for UFG and CG Ni at different strain levels. It can be seen that, with increasing macroscopic strain, the residual ε_{II}^{200} for the UFG Ni samples increase in TD but decrease in LD. Figure 2(b) compares ε_{II}^{200} of NC, UFG, and CG Ni at 2% strain level, where the abnormal behavior of ε_{II}^{200} (compressive in LD) in the UFG regime is clearly demonstrated. This result shows that ε_{II}^{hkl} of UFG Ni was significantly relaxed in LD, suggesting that other deformation mechanisms are also operating in the UFG regime.

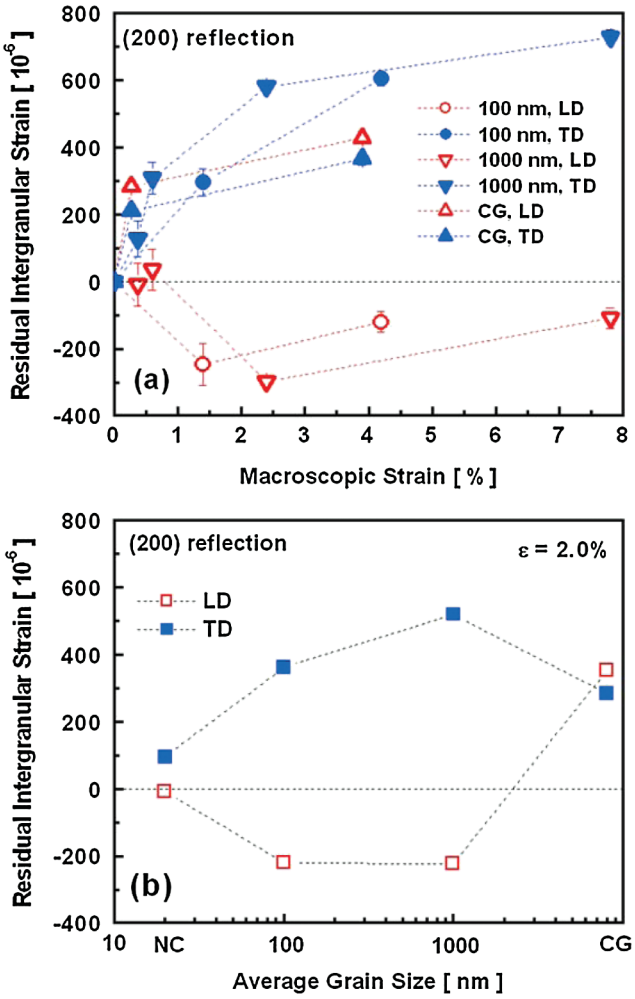

FIG. 2 (color). (a) A summary of the (200) residual intergranular strains (upon unloading) in Ni samples with different grain sizes. (b) The (200) residual intergranular strains as a function of the grain size at 2% strain, which were estimated from Fig. 2(a) by interpolation. In UFG samples, while significant intergranular strains were found, their behaviors in longitudinal (red color) and transverse (blue color) directions are different, demonstrating that other deformation mechanisms are also operating in the UFG regime.

It has been established that deformation twins can effectively relieve or even reverse ε_{II}^{hkl} in LD [22,23]. To search for evidence of twinning, we conducted extensive TEM examinations of all of our Ni samples after *in situ* tensile testing. For the NC sample, little microstructure change was detected, with no apparent evidence of a dislocation network or twinning after a 2% plastic strain, consistent with previous TEM studies [24]. In UFG Ni samples, however, both dislocations and extensive deformation twins were observed. Figure 3(a) shows the microstructure of sample *B* after subjecting to ~6% tensile strain. Both dislocation activities (e.g., indicated by the arrows) and deformation twins can be readily seen. Similar features were found in UFG sample *C*. In the CG Ni sample, only dislocations were observed, as expected. Over the large number of UFG grains (>1000) examined, the deformation twins were more likely to appear in the larger grains than in the smaller ones. This is illustrated by Fig. 3(b), where the fraction of UFG grains containing deformation twins is plotted as a function of the grain size. From these TEM observations, clearly twinning plays a significant role in the deformation of UFG Ni. The observed reversal of residual strains in LD is consistent with deformation twinning. It is also noteworthy that an unusual ε_{II}^{hkl} and deformation twinning were observed in UFG Ni subjected to cyclic loading [25].

Discussions.—The lack of ε_{II}^{hkl} and texture development in sample *A* indicates GB-mediated plastic deformation in NC Ni. Coble creep is a well-known GB-mediated deformation mechanism, but this typically happens at high temperature, where the materials exhibit low strength and high rate sensitivity [26,27]. Our experiment was conducted at room temperature under quasistatic loading condition, where the sample reached a high strength of more than 1 GPa. Thus, the GB-mediated plastic deformation seen here cannot be attributed to Coble creep.

Leading theories by MD simulations predicted several deformation mechanisms, such as GB sliding [2–4] or emission of partial dislocations from GBs [5]. However,

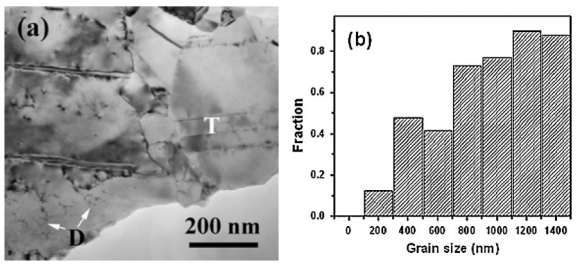

FIG. 3. (a) Microstructure of UFG sample *B* after subjecting to ~6% tensile strain, where both dislocation activities (*D*) and deformation twinning (*T*) are evident. (b) Fraction of grains containing deformation twins as a function of the grain size.

these simulations were carried out for deformation at short time scales, corresponding to very high strain rates, and the ensembles were limited to only a few grains. For this reason, the simulation results cannot be directly compared with diffraction data collected during *in situ* quasistatic loading and averaged over the entire scattering volume. Future studies are necessary to bridge the gap between experiments and theories, and to determine unambiguously the deformation mechanisms in the NC regime.

With high stacking fault energy, CG Ni is not known to deform via twinning except under extreme conditions (e.g., shock wave loading) [28]. An analysis involving the generalized planar fault energy curve indicates that the deformation in NC Ni could be carried out by stacking faults under tensile loading, but twinning is unlikely, due to the high-energy barrier [5]. On the other hand, Zhu *et al.* argued that in NC samples, a stacking fault may be converted to a twinning nucleus, and predicted an optimum grain size where twins can readily form [29]. Recent TEM studies on Ni samples subjected to severe deformations (e.g., low temperature and high strain rate) provided experimental evidence supporting this argument [30–32]. The present study demonstrates that under a quasistatic loading condition, deformation twinning can also take place, but at larger grain sizes in the UFG regime. As Fig. 3 shows, the propensity of deformation twinning increases with the grain size, similar to what Zhu *et al.* found in NC samples under severe deformation conditions. However, as the grain size further increases to the CG regime, the propensity of twinning will eventually vanish. Thus, twinning is a competitive deformation mechanism when the grain size becomes sufficiently small (e.g., in submicrons). Whether or not a twin occurs depends on the deformation condition and the grain size. As an important deformation mechanism, twinning must be taken into account in further theoretical development on size-dependent deformation behaviors.

Concluding remarks.—In summary, size-dependent deformation behaviors are revealed over a broad range of grain sizes by *in situ* synchrotron and neutron diffraction. As the grain size is reduced to the UFG regime, twinning becomes competitive. In the NC regime, the deformation is mediated by GB activities. Our results brought to light new findings not accessible by other experimental probes. While the focus of this study is NC and UFG Ni, the methodology is applicable to other materials systems and is expected to play an important role in fundamental study of deformation at small length scales.

The authors thank Dr. E. Ma for helpful discussions. This research was supported by U.S. Department of Energy (DOE), Office of Basic Energy Sciences, under Contract No. DE-AC05-00OR22725 with UT-Battelle, LLC. Use of APS was supported by the U. S. DOE under Contract No. DE-AC02-06CH11357. This work has benefited from the use of the Lujan Neutron Scattering Center at LANSCE, which is funded by the US DOE, Office of Basic Energy Sciences under Contract DE AC52 06NA25396. L. Z. and X. L. W. thank Natural Science Foundation of China for supporting their collaborative research (No. 50528102).

*wangxl@ornl.gov

[1] J. R. Weertman *et al.*, MRS Bull. **24**, 44 (1999).
[2] J. Schiotz, F. D. Di Tolla, and K. W. Jacobsen, Nature (London) **391**, 561 (1998).
[3] J. Schiotz and K. W. Jacobsen, Science **301**, 1357 (2003).
[4] H. Van Swygenhoven and P. M. Derlet, Phys. Rev. B **64**, 224105 (2001).
[5] H. Van Swygenhoven, P. M. Derlet, and A. G. Froseth, Nature Mater. **3**, 399 (2004).
[6] K. S. Kumar, H. Van Swygenhoven, and S. Suresh, Acta Mater. **51**, 5743 (2003).
[7] M. Chen *et al.*, Science **300**, 1275 (2003).
[8] X. Z. Liao *et al.*, Appl. Phys. Lett. **83**, 5062 (2003).
[9] S. Cheng, J. A. Spencer, and W. W. Milligan, Acta Mater. **51**, 4505 (2003).
[10] V. Yamakov *et al.*, Nature Mater. **3**, 43 (2004).
[11] Z. Budrovic *et al.*, Science **304**, 273 (2004).
[12] J. R. Trelewicz and C. A. Schuh, Acta Mater. **55**, 5948 (2007).
[13] A. S. Argon, *Strengthening Mechanisms in Crystal Plasticity* (Oxford University Press, New York, 2008), pp. 64.
[14] H. Li *et al.*, Phys. Rev. Lett. **101**, 015502 (2008).
[15] A. S. Argon, *Strengthening Mechanisms in Crystal Plasticity* (Oxford University Press, New York, 2008), pp. 154.
[16] S. Cheng *et al.* (unpublished).
[17] J. W. L. Pang *et al.*, Acta Mater. **48**, 1131 (2000).
[18] B. Clausen, *Characteristics of Polycrystalline Deformation by Numerical Modeling and Neutron Diffraction Measurements*, ResøNational Laboratory Report, 1997, ISBN 87-550-2304-5.
[19] B. Clausen, T. Lorentzen, and T. Leffers, Acta Mater. **46**, 3087 (1998).
[20] Y. D. Wang *et al.*, Nature Mater. **2**, 101 (2003).
[21] J. W. L. Pang, R. B. Rogge, and R. L. Donaberger, Mater. Sci. Eng. A **437**, 21 (2006).
[22] D. W. Brown *et al.*, Mater. Sci. Eng. A **399**, 1 (2005).
[23] B. Clausen *et al.*, Acta Mater. **56**, 2456 (2008).
[24] X. L. Wu, Y. T. Zhu, and E. Ma, Appl. Phys. Lett. **88**, 121905 (2006).
[25] S. Cheng *et al.*, Acta Mater. **57**, 1272 (2009).
[26] R. J. Coble, J. Appl. Phys. **34**, 1679 (1963).
[27] V. Yamakov *et al.*, Acta Mater. **50**, 61 (2002).
[28] J. A. Venables, in *Deformation Twinning*, edited by R. E. Reed-Hill, J. P. Hirth, and H. C. Rogers (Gordon & Breach, New York, 1964), pp. 77–116.
[29] Y. T. Zhu *et al.*, J. Appl. Phys. **98**, 034319 (2005).
[30] E. M. Bringa *et al.*, Science **309**, 1838 (2005).
[31] X. L. Wu, Y. Qi, and Y. T. Zhu, Appl. Phys. Lett. **90**, 221911 (2007).
[32] X. L. Wu and Y. T. Zhu, Phys. Rev. Lett. **101**, 025503 (2008).